



TECHNICAL UNIVERSITY OF CLUJ-NAPOCA

ACTA TECHNICA NAPOCENSIS

Series: Applied Mathematics, Mechanics, and Engineering  
Vol. 67, Issue Special I, February, 2024

## EXPLORING FRONTAL IMPACT BEHAVIOR AND ABSORBED ENERGY OF A NOVEL CAR BUMPER BEAM CONSTRUCTION SOLUTION

Robert-Marian BLEOTU, Cosmin PREDA, Valentin Ștefan OLEKSIK

**Abstract:** The safety of human lives is put in danger by car accidents around the globe. Thus, the implementation and creation of important safety elements is one of the top priorities of car manufacturing companies. Unfortunately, the statistics do not provide promising results in this regard and a lot of attention, from both engineers and researchers, is dedicated to the safety elements of the motor vehicle. This work aims to study the dynamic impact behavior of the metallic front bar used in the construction of motor vehicles. In order to create a new constructive solution for the metal bar, characteristics such as longitudinal shape, bending angle, bending radius, perforation of the front plate, and thickness were studied with the help of finite element simulation. Finally, a comparison analysis was made between such a metal bar, used on one of the safest vehicles, and a novel prototype. We demonstrate that the prototype has the best results in terms of deformation and energy absorption.

**Key words:** metal front bar, absorbed energy, origami engineering, finite element analysis, lightweight materials, dynamic analysis, safety.

### 1. INTRODUCTION

Due to the rapid development of technology and human beings evolution, the number of cars purchased is continuously increasing. Together with this increase, the number of road accidents that lead to the injuries or even death of car drivers and passengers also increases [1]. Thus, the safety offered by the vehicle has become a subject of interest for multiple engineers and researchers [2]. For impact resistance verification, in the 1970s, car manufacturers introduced physical testing [3-5]. As technology developed, finite element simulations replaced physical testing reducing the production costs. Thus, there is no longer any need to destroy vehicles or their various components [6-9].

Another goal of car manufacturers is to replace heavy materials (steel) with light materials (aluminum, magnesium, and their alloys). This is due to the current world trend to produce lighter, greener, cheaper, and safer vehicles [10]. The challenges of improving safety and at the same time reducing greenhouse gas emissions have become a priority objective

for vehicle manufacturers [11]. Following the study of Jurgen et al. [12], it was concluded that aluminum alloys reduce weight by 50%. This is achieved without compromising the strength, safety, and performance of the vehicles. These alloys offer very good mechanical properties, such as high strength in relation to weight, tensile strength, corrosion resistance, thermal and electrical conductivity [11].

The metal front bumper is used in the automotive industry to absorb energy in the event of an impact. It is located by means of screws in the front part of the vehicles. The design of this component must be done with the aim of reducing the damage caused by a collision.

The capacity of the metal bar under impact loads is called impact strength. Thus, through better deformation performance, the effect of the accident is reduced. The energy is absorbed by this component in a certain amount that differs according to the characteristics of each metal bar model.

The remaining energy propagates through the other components, thus it is completely or

partially dissipated. The energy dissipation effect can lead to saving human lives or avoiding injuries [13]. Another role of the bumper is to protect the more fragile mechanical components positioned behind it [14].

In recent years, due to the desire to reduce the weight of vehicles, many studies have been carried out on the material science from which these components are made. One of the materials studied and used in the production of metal front bars was high strength steel. It offers impact resistance and high durability, but it has the disadvantage of high weight [15]. On the one hand, aluminum and magnesium alloys are also used in the production of these components. The main advantage of aluminum alloys is represented by its ability to absorb energy.

Another advantage of this material is its high deformation capacity using low stress levels. Magnesium alloys have been used too due to their improved weight reduction [16].

On the other hand, composite materials have been studied for use in automotive safety components. They have advantages such as high specific strength, high specific stiffness and corrosion resistance. It also presents limitations and disadvantages namely high cost, environmental sensitivity, low damage tolerance, a time-consuming manufacturing process, and limited strength in the perpendicular direction of the fiber [15].

The "Origami Engineering" technique offers a special interest among engineers. Researchers have discovered that the simple folding of paper can be easily adapted to the construction of new material structures [17].

The materials for which this technique is especially suitable are metal sheets, plastic or carbon fiber. They help to achieve strong, light structures with very good energy absorption properties [18].

Research studies have been focused on the use of this technique in the construction of motor vehicles. It has been demonstrated that thin-walled origami tubes play an important role in energy absorption. The tubes studied were tubes with hexagonal section [19], tubes with circular section [20], tubes with square section [21], tubes with section triangular [22] and tubes with hybrid section [23].

## 2. METHOD

### 2.1 The position of the bumper in the strength structure of vehicle

The bumper is part of the resistance structure of motor vehicles. It is positioned at the front and is fixed with screws to the side members. Figure 1 presents the position that this component occupies in the frontal safety assembly of the motor vehicle. The bumper is part of an assembly of four components: bumper fascia, energy absorber, bumper beam, and side member.

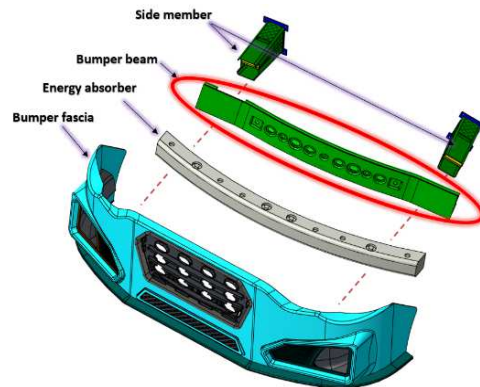


Fig. 1. Bumper system.

This assembly has the role of dissipating energy in the event of a collision. In Figure 2 it is showed the path of energy dissipation through the resistance structure of vehicles.

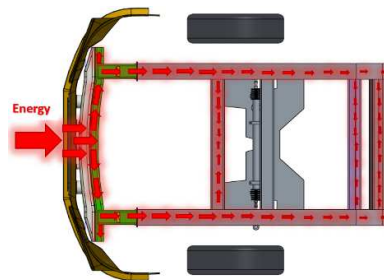


Fig. 2. Energy dispersion through the resistance structure.

### 2.2 3D models

The Creo Parametric 3.0 M120 program was used to create the 3D models. The 3D models have been categorized in metal profiles, tubes and bumpers to improve the finite element simulations.

### 2.2.1 Metal profiles

Metal sheets were divided according to their studied characteristics such as longitudinal shape, bending angle, bending radius and plate perforation. Their length is fixed at 1500 mm, and the cross-section has the shape of a square with a side of 100 mm. Figure 3 illustrates four profile variants which will be study in this work, namely profile with different longitudinal shape: rectilinear, radius, and angle (i), with different bending angle: 145°, 160°, 175° (ii), with different bending radius: R1500, R3000, R5000 (iii) and with or without punching (iv).

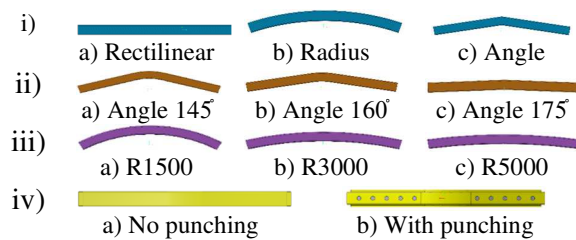


**Fig. 3.** The 3D models for the longitudinal shape (i), the bending angle (ii), the bending radius (iii) and the material with and without punching (iv).

### 2.2.2 Thin-walled tubes

Following the conducted research, it was concluded that the tube with a hexagon-shaped cross-section has a very good capacity to absorb energy. Thus, the 3D model for two thin-walled tubes was made. One in vertical position and the other in horizontal position. They have a height of 60 mm, the side of the hexagon is 35 mm and the thickness is 1 mm. The two variants can be seen in Figure. 4.

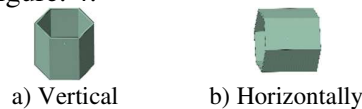


**Fig. 4.** Thin-walled tubes design.

### 2.2.3 Bumper beam

In order to obtain the final results of the study, two constructive versions of the bumper were made. A first version, which is used as a comparison model and a second version, which contains all the favorable parameters that were analyzed. These bumpers consist of two sheets welded together. Their length is 1500 mm. The two bar variants are represented in Figure 5.



**Fig. 5.** Bumper beam.

Figure 6 shows the component elements that are part of the bumper assembly that contains all the improvement elements studied. It is composed of an embossed sheet (back element), thin-walled tubes and a folded and perforated sheet on the front surface (front element). During the course of this study, the tubes were situated both in the center and on the sides of the bumper beam. Consequently, this configuration left two areas uncovered by the tubes. This choice was influenced by the fact that the majority of collisions typically transpire in the regions where the tubes were positioned. In forthcoming research, we will endeavor to encompass the complete surface of the bumper beam by utilizing thin-walled tubes.

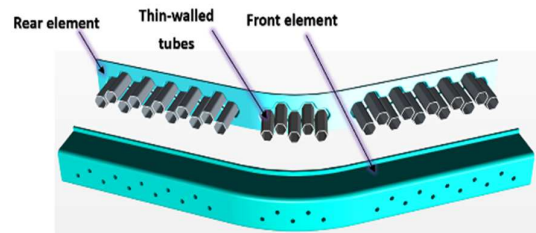


**Fig. 6.** Bumper beam components.

### 2.3 Finite element analysis (FEA)

Finite element analyzes were performed using the Abaqus program. The material used for the element analysis was Aluminum 6063. Table 1 shows the mechanical properties of this material.

*Table 1*

**Mechanical properties – Aluminum 6063**

Mechanical properties	Value
Density [kg/m <sup>3</sup> ]	2700
Young modulus (GPa)	70
Yield Strength (MPa)	214
Tensile Strength (MPa)	271
Poisson's Ratio	0.33

#### 2.3.1 Dynamic analysis of metal profiles

To obtain the results, the body of each constructive profile variant was embedded at the ends at a distance of 200 mm. We simulate the interaction of a rigid body with a speed of 10 m/s with the variant. Figure 7 presents the input data for the four profile data sets.

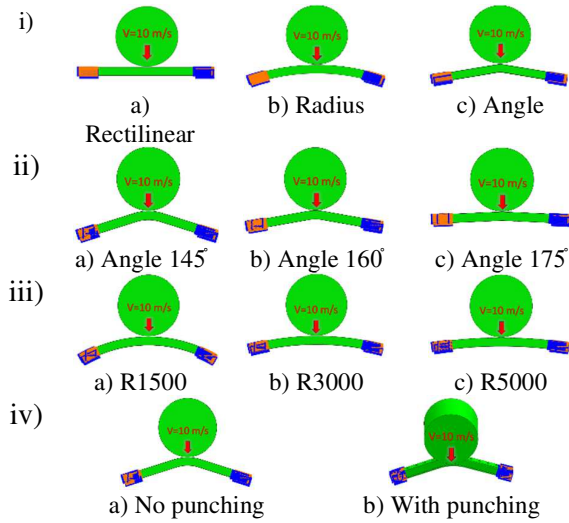


**Fig. 7.** Input data for longitudinal shape (i), the bending angle (ii), the bending radius (iii) the material with and without punching (iv).

### 2.3.2 Static analysis of thin-walled tubes

In order to obtain the final results, the two variants of the hexagonal tube were subjected to a displacement. The displacement applied to the first variant was carried out in the direction of the Z axis, and its embedment was positioned on the end of the tube. The displacement applied to the second tube variant was carried out in the direction of the Y axis, and the embedment was carried out on the surface of a side face.

### 2.3.3 Static analysis of bumpers beam

After the modeling of the two bar variants, the preparation of the input data for the finite element simulation was carried out. Both variants were subjected to a displacement of -106 mm in the X direction. Their embedment was carried out at the ends of the bars at a distance of 200 mm. Figure 8 shows the preparation of the input data for the two constructive variants of the front metal bar.

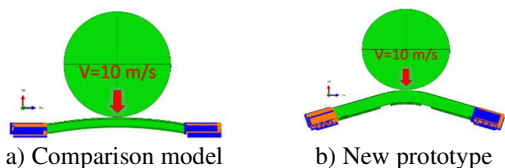


**Fig. 8.** Input data preparation for the bumper beam.

## 3. RESULTS

In this chapter, the results obtained from finite element analyzes. The targeted results were related

to the deformations, stresses and displacements of the material. The comparison of the results in terms of energy absorption in time was possible with the help of the graphs obtained from the analyzes carried out. In the analysis, the maximum allowable stress value of the material, 271 MPa, was also introduced, with the intention of conducting the analysis until the point of failure. The purpose of the analysis was to determine the absorbed energy and not the manner in which the material fractures.

### 3.1 Results – metal profiles

Following the dynamic analyzes performed, the comparative results obtained for each characteristic of the metal profiles, in the most suitable case.

#### 3.1.1 Metal profiles – longitudinal shape

Figure 9 shows the results obtained for the longitudinal profile based on plastic strain (i), stress (ii) and material displacement (iii). Due to the effective plastic strains occurring in the material, small details of the materials can be observed in the contact area and in the profile embedding area. The maximum stresses resulting from the impact gradually decrease from the contact area towards the ends of the three profiles. The angled metallic profile indicates the highest material surface and stress compared with the other 2 analyzed profiles.

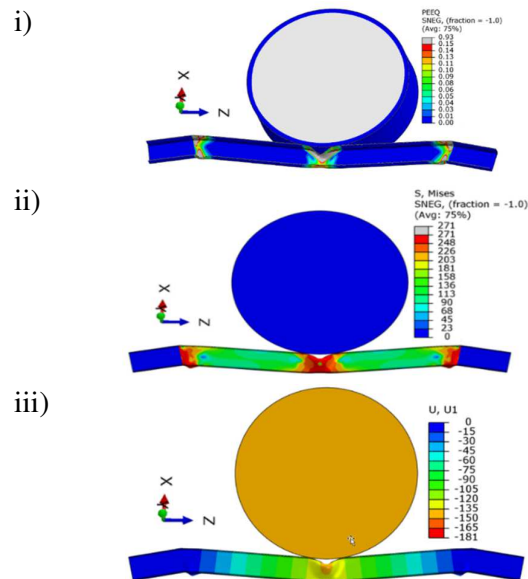


**Fig. 9.** Effective plastic strain (i), stress (ii), displacement (iii) results for longitudinal shape - angle case.

The angle profile acquired the highest material displacement, being beneficial to energy absorption. Close to the displacement result of this profile was also the result of the radius profile.

Figure 10 shows the Energy/Time graph. From this comparative analysis we can draw the conclusion that the profile, which contains an angle, is the best variant in terms of the ability to deform plastically, absorbing a considerable amount of energy. The metal profiles have an approximately identical route with respect to the energy absorption, but the straight profile stops absorbing energy in the time interval 0.02-0.03[s], while the others continue to absorb energy, stabilizing at a low absorption value (500 J).

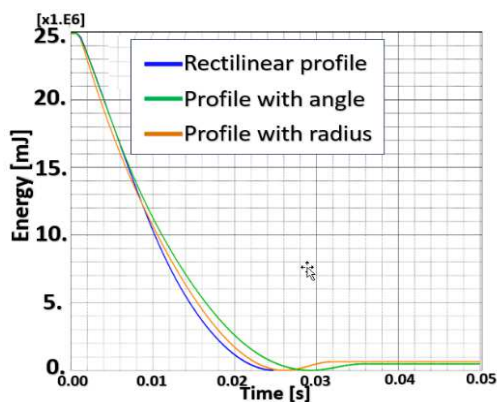


Fig. 10. Graph Energy/Time dependence for the longitudinal shape.

### 3.1.2 Metal profiles – bending angle

From Figure 11 you can see the results related to the profile containing the angle of 145 degrees. Thus, following this analysis, effective plastic strain (i), tension (ii) and material displacement (iii) are presented.

Unlike the other two profiles, the 145° angle profile contains less profile destruction due to movement in both sides, the center and recess areas.

The profile with the largest bending angle is favored with respect to the surface covered by high stresses. The displacement of the material that occurs following the impact was different for the analyzed profiles.

The largest displacement was found at the 160° profile (-178 mm), followed by the 145° profile (-163 mm).

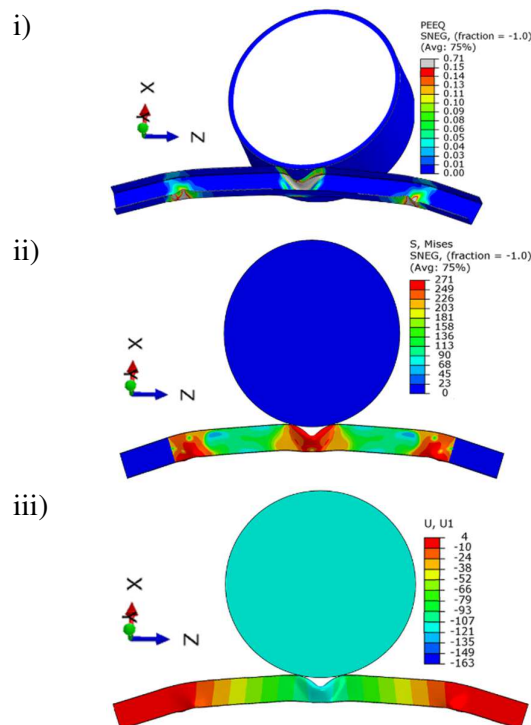


Fig. 11. Effective plastic strain (i), stress (ii), displacement (iii) results for bending angle - the 145° case.

From the comparative analysis it is concluded (see Fig. 12) that all three metal profiles have close results in terms of energy absorbed over time. The advantage that differentiates the profile with the angle of 145° is made by the shorter time in which the amount of energy is absorbed.

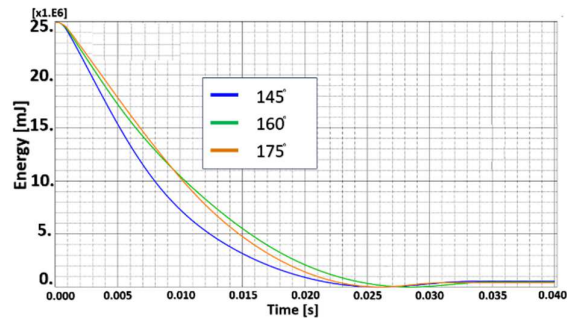
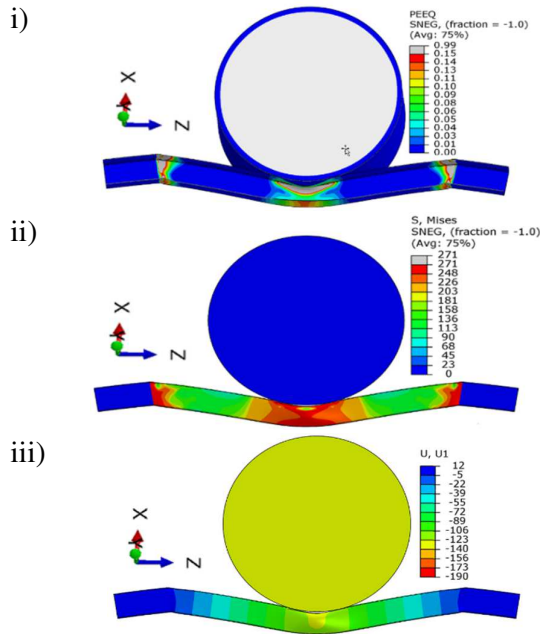


Fig. 12. Graph Energy/Time as a function of bending angle.

### 3.1.3 Metal profiles - bending radius

Figure 13 presents the results for the profile with a radius of 5000 mm with respect to the effective plastic strain of the material (i), the tension (ii) and the displacement that occurs following the impact with the rigid body (iii). The high values of the effective plastic strain are particularly noticeable in the profile with a

radius of 5000 mm. The deformations are found in the central area and in the profile extremes. These areas were also affected in the other two profiles that contain different radii. However, the effective plastic strain was less. The maximum stress in the material (iii) has the smallest area compared to the rest of the analyzed profiles. This is especially evident at the ends of the profiles.



**Fig. 13.** Effective plastic strain (i), stress (ii), displacement (iii) results for bending radius of 5000 mm.

Figure 14 shows the Energy/Time graph for the three metal profile variants with different bending radii. It can be seen that the profile with a radius of 5000 mm has a higher absorption speed than the other two, thus it is considered the most favorable result. The 3000 mm radius profile has values close to it. They stabilize in the time interval 0.03-0.04 s.

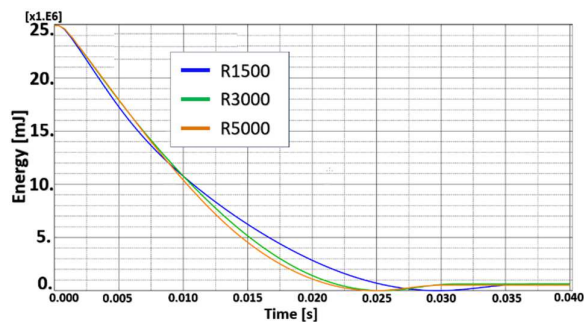


**Fig. 14.** Graph Energy/Time as a function of bending radius.

### 3.1.4 Metal profiles - punching

Figure 15 presents the results of the metal profiles that have as a differentiating element the punching of the surface or its absence. Following the analysis, effective plastic strain (i), tension (ii) and material displacement (iii) were highlighted. As it can be seen, the effective plastic strain of the punching profile is spread over a larger area, compared to the non-punching profile where the phenomenon of material wrinkling occurs. Also, the maximum stress dissipation occurs towards the ends of the profile. Regarding material movement, the profile without punching on the front surface have the largest movement compared to the other analyzed profile.

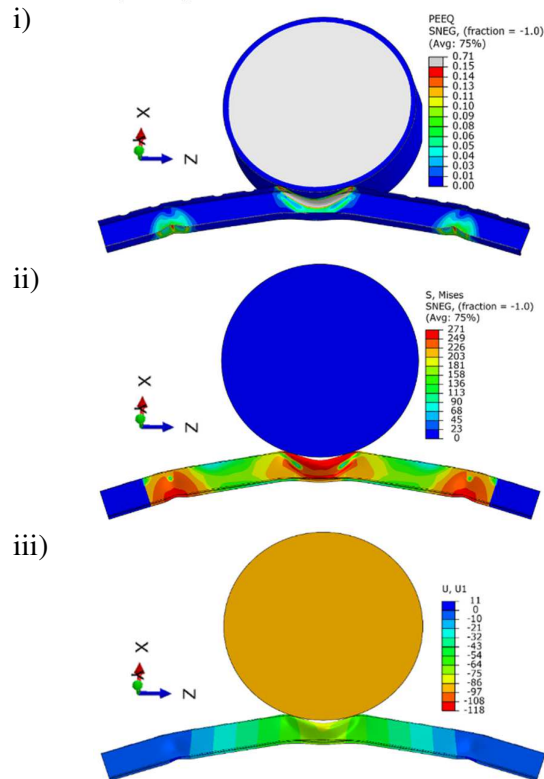


**Fig. 15.** Effective plastic strain (i), stress (ii), displacement (iii) results for the punching profile.

From the comparative analysis it is concluded (see Fig. 16) that perforation brings a considerable improvement in terms of energy absorption thus, the energy resulting from the impact was absorbed faster compared to the profile without perforation.

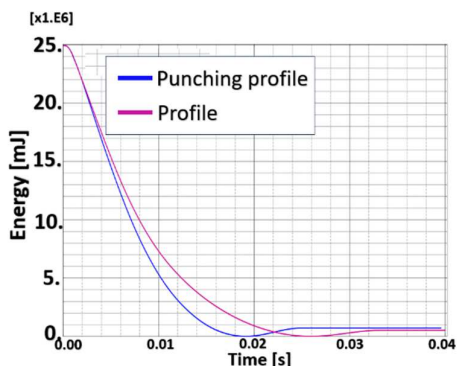


Fig. 16. Graph Energy/Time depending on the punching.

Table 2 shows the results obtained from the dynamic analyzes performed on the different characteristics of the metal profiles.

Table 2

Results – metal profiles		
	Effective plastic strain [%]	Displacement [mm]
<b>Rectilinear</b>	128	-139
<b>Radius</b>	75	-161
<b>Angle</b>	93	-181
<b>Angle 145°</b>	71	-163
<b>Angle 160°</b>	70	-178
<b>Angle 175°</b>	119	-153
<b>R1500</b>	52	-190
<b>R3000</b>	46	-190
<b>R5000</b>	99	-190
<b>No punching</b>	71	-163
<b>Whit punching</b>	71	-118

### 3.2 Results – thin-walled tubes

Following the static analyzes performed, comparison results were obtained for the two thin-walled tube variants. The element of differentiation in them is made by the direction of movement to which they are subjected.

Figure 17 shows the effective plastic strain (i), the areas with maximum and minimum stresses appearing in the material (ii) and the displacement resulting from the analysis for the two tube variants (iii). The tube under stress, in the Z-axis direction, forms a loop of material with the largest deformation area.

As for the stresses arising in the material, they dissipate from the tightening of the material towards the ends of the tube. In the case of the tube stressed in the direction of the radius, the maximum stresses occurred at the corners of the tube and dissipated towards the side faces. The largest displacement of the material was found in the radially stressed tube.

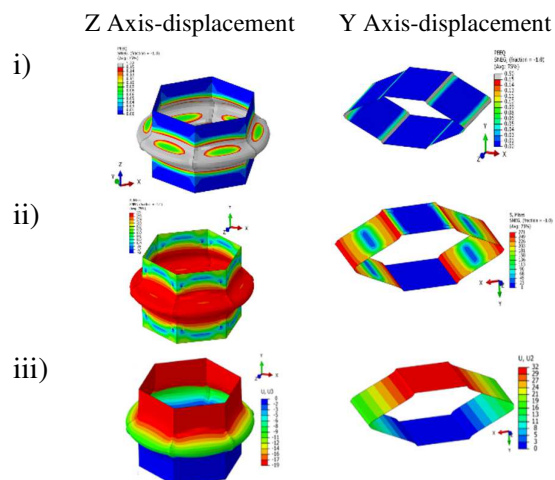


Fig. 17. Effective plastic strain (i), stress (ii), displacement (iii) results for thin-walled tubes.

Figure 18 presents the Energy/Displacement graph. From this comparative analysis, it can be concluded that the tube placed in a vertical position has a much greater capacity to absorb energy at the moment of stress than the tube positioned in a horizontal position.

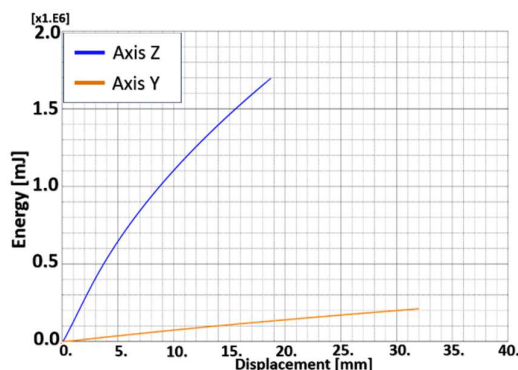


Fig. 18. Graph Energy/Displacement for the thin-walled tubes.

Table 3 shows the results obtained for the two tube variants.

Table 3

Results – thin-walled tubes		
	Z axis	Y axis
Effective plastic strain [%]	122	50
Displacement [mm]	-19	-32
Energy [J]	1700	210

### 3.3 Results – bumper beam

The two constructive variants of the bar were subjected to static analyzes. These were

simulated for a displacement of -106 mm on the X axis.

Figure 19 shows the results obtained for the new prototype in terms of effective plastic strain (i), stress (ii) and material displacement (iii). The most affected area by the effective plastic strain of the material is identified at the level of the origami structure that is in the contact area with the rigid body. Unlike the new prototype, the comparison model shows a high percentage of effective plastic strain along the entire length of the profile. The maximum stresses of the new prototype are found at the level of the metal profile, both in the stressed area and at the ends of the profile. The cells do not have very high stress. The maximum material displacements were identified at the central core level.

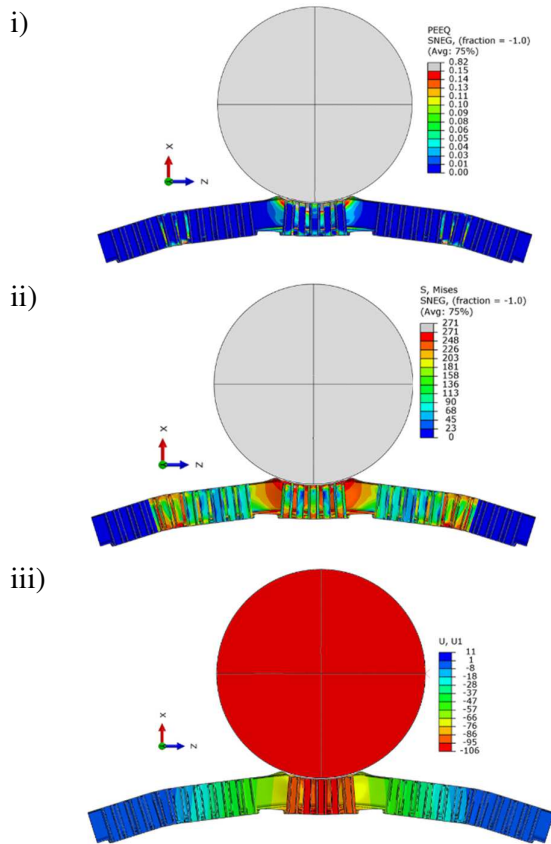


Fig. 19. Effective plastic strain (i), stress (ii), displacement (iii) results for the new prototype.

Figure 20 shows the Energy/Time graph. After consulting the graph, it can be seen how the origami core bumper has a better energy absorption capacity compared to the metal front bumper used as a comparison model.

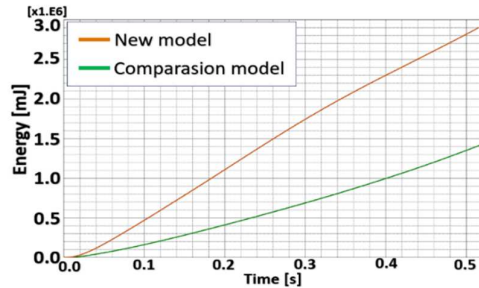


Fig. 20. Graph Energy/Time – Bumper beam.

Table 4 presents the results obtained for the two versions of the bumper.

Table 4

Results – bumper beam		
	Comparison model	Novel prototype
Effective plastic strain [%]	61	82
Displacement [mm]	-106	-106
Energy [J]	2900	1400

#### 4. CONCLUSION

Passenger safety is the highest priority of engineers and researchers. Thus, this work aimed to improve one of the most essential components in terms of passenger safety. In this paper, finite element simulations were conducted to enhance the energy absorption capabilities of the bumper beam used in automobile construction. To achieve this goal, simulation analyzes were performed on various design features of these bumpers. The characteristics analyzed were: longitudinal shape, bend angle, bend radius, material perforation, thin-walled tubes and the final bumper assembly. Thus, the following conclusions were reached:

- The metal profile with an angle and the one with a bending radius obtained the most favorable results with respect to the absorption energy in favor of the rectilinear profile;
- The profile with an angle of 145° and the one with a radius of 5000 mm absorb the largest amount of energy, unlike the other analyzed profiles in their category;
- The perforation of the front surface of the profile improves energy absorption

- Thin-walled tubes have a greater energy absorption capacity when they are axially stressed;
- The new prototype, which contains all the analyzed characteristics, absorbs a much higher amount of energy than the comparison model used;
- The Origami Engineering technique has also proven in this case to be a very good solution for improving energy absorption.

## 5. REFERENCES

- [1] Idrees, U., Ahmad, S., Talha, M., Shehzad, R., *Finite element analysis of car frame frontal crash using lightweight materials*, Journal of Engineering Research, 11(1), 2023.
- [2] Aydin, M.M., *The modeling of effective parameters on public bus passengers' boarding time prediction*, Journal of Engineering Research, 10(1B), 2022.
- [3] Ali, F.N., Roozbeh, A., Mozafar, S.R., Mohd, Y.Y., Seyed, S.R.K., Michal, P., *Using Finite Element Approach for Crashworthiness Assessment of a Polymeric Auxetic Structure Subjected to the Axial Loading*, Polymers, 12(6), 2020.
- [4] O'Malley, S., Zubby, D., Moore, M., Paine, M., Paine, D., *Crashworthiness Testing of Electric and Hybrid Vehicles*, International Technical Conference on the Enhanced Safety of Vehicles (ESV) National Highway Traffic Safety Administration, April 2015, Göteborg.
- [5] Borovinsek, M., Vesenjajk, M., Ulbin, M., Ren, Z., *Simulation of crash tests for high containment levels of road safety barriers*, Engineering Failure Analysis, 14, 1711-1718, 2007.
- [6] Fathalla, A.S.M., Akhavan, F.A., Moezzi, R., Kolor, S.S.A., *A Numerical Study of the effect of Bolt Thread Geometry on the Load Distribution of Continuous Threads*, Journal of Engineering Research, 10(2B), 2022.
- [7] Wonjoon, K., Taebeum, R., Donggun, R., Myung, H.Y., *Analysis of customers' satisfaction with automobile exterior panel stiffness: focus on the hood and doors of mid-sized sedan*, Journal of Engineering Research, 7(2), 2019.
- [8] Cheng, W., *Design of helical gear transmission systems with high power density*, Journal of Engineering Research, 6(4), 2018.
- [9] Bertan, B., *Design and discrete optimization of hybrid aluminum/composite drive shafts for automotive industry*, Journal of Engineering Research, 9(3B), 2019.
- [10] Blawert C., Hort N., Kainer K.V., *Shape optimization of beams under transverse crash*, Transactions of the Indian Institute of Metals, 57, 2004.
- [11] Zhang, W., Xu, J., *Advanced lightweight materials for Automobiles: A review*, Materials & Design, 221, 2022.
- [12] Hirsch, J., *Aluminium in innovative lightweight car design*, Material transactions, 52(5), 2011.
- [13] Niyazi T., *Automotive applications of magnesium and its alloys*, The 15th International Conference on Machine Design and Production, June 2012, Denizli.
- [14] Natarajan, N., Joshi, P., Tyagi, R., *Design improvements of vehicle bumper for low speed impact*, Materials Today: Proceedings, 38(1), 2021.
- [15] Du, B., Li, Q., Zheng, C., Wang, S., Gao, C., Chen, L., *Application of Lightweight Structure in Automobile Bumper Beam: A Review*, Materials, 16(3), 2023.
- [16] Joshi, V.V., Jana, S., Li, D., Garmestani H., Nyberg, E., Lavender, C., *High shear deformation to produce high strength and energy absorption in Mg alloys*, Magnesium Technology 2014, 2014.
- [17] Xiang, X.M., Lu, G., You, Z., *Energy absorption of origami inspired structures and materials*, Thin-Walled Structures, 157, 2020.
- [18] You, Z., *Folding structures out of flat materials*, Science, 345(6197), 2014.
- [19] Yin, J., Wang, Z., Liao, W., Hong, L., Ding, Y., Zhou, Z., *A data fusion based diagnostic methodology for in-situ debonding detection in beam-like honeycomb sandwich structures with fiber Bragg grating sensors*, Measurement, 191, 2022.

- [20] Ha, N.S., Pham T.M., Tran, T.T., Hao, H., Lu, G., *Mechanical properties and energy absorption of bio-inspired hierarchical circular honeycomb*, Composites Part B, 236, 2022.
- [21] Singh, R., Rashid F.M., *Numerical investigation on the effect of different face sheet materials and core designs on the ballistic response of sandwich structures under low-velocity impact*, Materials Today: Proceedings, 56, 2022.
- [21] Xiang, X.M., Lu, G., You, Z., *Energy absorption of origami inspired structures and materials*, Thin-Walled Structures, 157, 2020.
- [22] Mallick, M., Chakrabarty, A., Khutia, N., *Genetic algorithm based design optimization of crashworthy honeycomb sandwiched panels of AA7075-T651 aluminium alloy for aerospace applications*, Materials Today: Proceedings, 54, 2022.
- [23] Chittappa, H., *Impact analysis of spiral cellular structured hybrid sandwiched panel using ANSYS explicit dynamics*, Materials Today: Proceedings, 52, 2022.

## EXPLORAREA COMPORTAMENTULUI LA IMPACT FRONTAL ȘI A ENERGIEI ABSORBITE A UNEI NOI SOLUȚII CONSTRUCTIVE A BAREI DE PROTECȚIE A MAȘINII

Rezumat: Siguranța vieților umane este pusă în pericol de accidente de mașină din întreaga lume. Astfel, implementarea și crearea unor elemente importante de siguranță este una dintre prioritățile de top ale companiilor producătoare de mașini. Din păcate, statisticile nu oferă rezultate promițătoare în acest sens și o mare atenție, atât din partea inginerilor, cât și a cercetătorilor, este dedicată elementelor de siguranță ale autovehiculului. Această lucrare își propune să studieze comportamentul dinamic la impact al barei frontale metalice utilizate în construcția autovehiculelor. Pentru a crea o nouă soluție constructivă pentru bara metalică, cu ajutorul simulării cu elemente finite au fost studiate caracteristici precum forma longitudinală, unghiul de îndoire, raza de îndoire, perforarea plăcii frontale și grosimea. În cele din urmă, a fost făcută o analiză comparativă între o astfel de bară metalică, folosită pe unul dintre cele mai sigure vehicule, și un prototip nou. Demonstrăm că prototipul are cele mai bune rezultate în ceea ce privește deformarea și absorbția de energie.

**Robert-Marian BLEOTU**, PhD Student, Eng., Lucian Blaga University of Sibiu, Faculty of Engineering, Machines and Industrial Equipment Department, robert.bleotu@ulbisibiu.ro, Romania.

**Cosmin PREDA**, PhD Student, Eng., Assistant, Lucian Blaga University of Sibiu, Faculty of Engineering, Machines and Industrial Equipment Department, cosmin.preda@ulbisibiu.ro, Romania.

**Valentin Ștefan OLEKSIK**, PhD. Eng., Professor, Lucian Blaga University of Sibiu, Faculty of Engineering, Machines and Industrial Equipment Department, valentin.oleksik@ulbisibiu.ro, Romania.